Spatial control of surface plasmon polariton excitation at planar metal surface

Zhichao Ruan,[1,2,*] Hui Wu,[3] Min Qiu,[2,4] and Shanhui Fan[5]

[1]*Department of Physics, Zhejiang University, Hangzhou 310027, China*

[2]*State Key Laboratory of Modern Optical Instrumentation, Zhejiang University, Hangzhou 310027, China*

[3]*State Key Laboratory of New Ceramics and Fine Processing, School of Materials Science and Engineering, Tsinghua University, Beijing 100084, China*

[4]*Department of Optical Engineering, Zhejiang University, Hangzhou 310027, China*

[5]*Ginzton Laboratory, Department of Electrical Engineering, Stanford University, Stanford, California 94305, USA*

**Corresponding author: zhichao@zju.edu.cn*

Received April 1, 2014; revised May 11, 2014; accepted May 14, 2014;
posted May 15, 2014 (Doc. ID 209263); published June 11, 2014

We illustrate that the surface plasmon polariton (SPP) excitation through the prism coupling method is fundamentally limited by destructive interference of spatial light components. We propose that the destructive interference can be canceled out by tailoring the relative phase for the different wave-vector components. As a numerical demonstration, we show that through the phase modulation the excited SPP field is concentrated to a hot energy spot, and the SPP field intensity is dramatically enhanced about three-fold in comparison with a conventional Gaussian beam illumination. The proposed phase-shaped beam approach provides a new degree of freedom to fundamentally control the SPP excitation and benefits the development of surface-enhanced applications.

OCIS codes: (240.6680) Surface plasmons; (240.0310) Thin films; (120.5060) Phase modulation; (230.6120) Spatial light modulators.

http://dx.doi.org/10.1364/OL.39.003587

Recently, particular attention has been attracted by using the spatial control techniques to control the excitation and concentration of light in a variety of optical systems. Vellekoop *et al.* demonstrated that sending light through a random scattering medium, with a spatially modulated input wavefront, can achieve the constructive interference at a focus spot, resulting in focusing beyond the diffraction limit [1]. This effect can be interpreted as time-reversal of light emitted from a point emitter [2]. A similar idea has also been applied to generate and control the location of light hot spots in a diffraction grating [3] and to experimentally focus surface plasmon wave on a metal surface of a nanohole array [4]. In another related work, Kao *et al.* proposed that in a plasmonic metamaterial the strong optically induced interactions between discrete metamolecules can be manipulated to realize a subwavelength scale energy localization through spatially tailoring the phase profile of a continuous-wave input light beam [5]. Conceptually, these spatial control methods have the strong analogy to the coherent control methods where an incident optical pulse is modulated in the time domain to steer light–matter interaction [6–8] or the response of optical systems [9–12] toward a desired final state.

Since a flat metal surface is the simplest geometry sustaining surface plasmons, it is of fundamental importance in plasmonics to efficiently excite the surface plasmon polariton (SPP) field on the surface [13]. The established excitation techniques, including the prism coupling method, have practical significance for applications including surface-enhanced sensing and spectroscopy [14,15], plasmonic nonlinear optics [16–18], and plasmon optical tweezers [19–21]. Here we propose that the SPP excitation on a flat metal surface can be dramatically enhanced by phase modulation of each wave-vector component of an incident light. We show that under a conventional illumination the spatial components of the incident light have destructive interference on the SPP excitation, and it strongly limits the SPP excitation and lowers the field intensity. We demonstrate that the destructive interference can be canceled out by shaping the illumination beam with a tailored relative phase for the different wave-vector components. As a consequence, the excited SPP field under the phase-shaped beam illumination is concentrated to a hot energy spot, and the electric field intensity is enhanced about three-fold at the peak in comparison with the conventional Gaussian beam illumination.

To clearly show the interference effect, we develop a spatial coupled-mode formula to model the SPP excitation process. To excite the SPP field at a metal-dielectric surface the prism coupling method of the Kretschmann and Otto configurations is commonly employed to satisfy the phase-matching requirement. Our theory can be generally applied to the prism coupling cases. As an example, here we consider a Kretschmann configuration [Fig. 1(a)], where a p-polarized incident beam illuminates a metal layer coating on a quartz prism. When the parallel component of the incident wave vector, k_z, is close to the SPP wave vector, the incident light excites SPP through the evanescent wave. Meanwhile the excited SPP leaks out and generates the radiation wave in quartz as it propagates along the z direction. Therefore, the reflection process consists of two pathways: the direct reflectance of the incident wave at the quartz-metal interface, and the outgoing radiation from the leakage of the excited SPP at the metal-air interface.

Based on the spatial coupled-mode theory (CMT) formalism [22], such an excitation process can be described by the following equations:

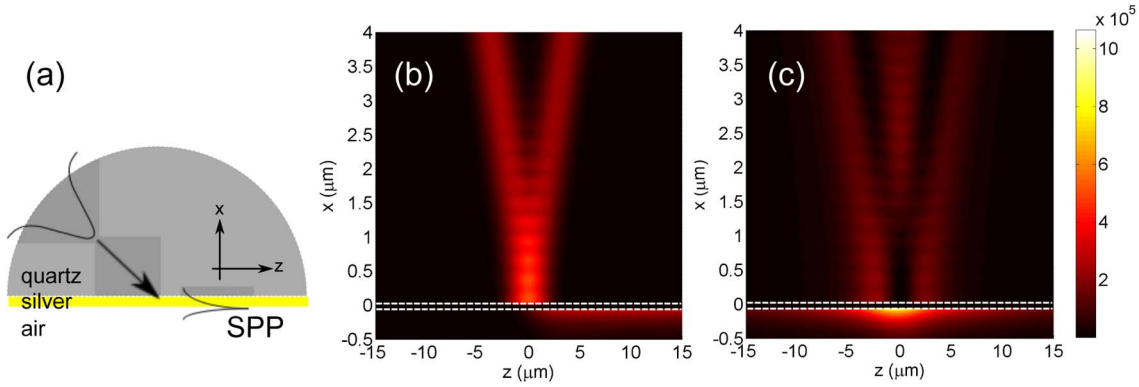

Fig. 1. (a) Schematic of a SPP excitation with the Kretschmann configuration. The thickness of the silver layer is 58.3 nm, and the dielectric constant of the quartz prism is $\varepsilon_d = 2.25$. (b),(c) Distribution of the electric field intensity $|\mathbf{E}|^2$ under the illumination of a Gaussian beam (b) and the phase-shaped beam (c). Here the white dashed lines outline the interfaces of the metal layer.

$$\frac{da}{dz} = (i\beta_{\text{spp}} - \alpha_l - \alpha_{\text{spp}})a + ie^{i\phi}\sqrt{2\alpha_l}S_{\text{in}}(z), \tag{1a}$$

$$S_{\text{out}} = e^{i\phi}S_{\text{in}} + ie^{i\phi}\sqrt{2\alpha_l}a. \tag{1b}$$

Here we take the convention that the field varies in time as $\exp(-i\omega t)$. a is the amplitude of the SPP, which is normalized such that $|a|^2$ corresponds to the time-averaged power along z direction. β_{spp} is the propagation constant of the SPP mode. $S_{\text{in}}(z)$ ($S_{\text{out}}(z)$) corresponds to the amplitude of the incident (reflective) light with the normalization of $|S_{\text{in}}|^2$ ($|S_{\text{out}}|^2$) giving the x-direction Poyntin flux. ϕ is the phase change of the reflection at the quartz-metal interface. α_l and α_{spp} correspond to the loss rate of the SPP due to the leaky radiation and that of the propagation loss due to intrinsic material absorption, respectively. Note that the spatial CMT takes the approximation of the strong confinement condition, i.e., $\alpha_l + \alpha_{\text{spp}} \ll \beta_{\text{spp}}$. We will see below in the numerical example that such an approximation is in fact sufficient for the SPP excitation at a real silver interface.

Let us consider two different scenarios with the spatial CMT theory. First, when the metal has an infinite thickness, the leaky rate $\alpha_l = 0$. In this case, Eqs. (1a) and (1b) are decoupled: the stable solution $a = \exp(i\beta_{\text{spp}}z - \alpha_{\text{spp}}z)$ of Eq. (1a) presents the SPP propagating in the z direction, and Eq. (1b) turns out as $S_{\text{out}} = e^{i\phi}S_{\text{in}}$, i.e., the reflected light solely experiences the phase change at the quartz-metal surface. In contrast, if the metal thickness is finite, Eq. (1a) shows the SPP excitation through the mode coupling. Equation (1b) indicates the reflective light contributed from the SPP excitation and the direct reflection at the quartz-metal surface. In this case, we expand the incident (reflected) beam into a series of plane waves as $S_{\text{in(out)}} = \int_{-\infty}^{\infty} s_{\text{in(out)}}(k_z)\exp(ik_z z)\mathrm{d}k_z$. On substituting into Eq. (1), the amplitude of the excited SPP and the reflection coefficient are obtained:

$$a(z) = \sqrt{2\alpha_l}e^{i\phi}\int_{-\infty}^{\infty}\frac{s_{\text{in}}(k_z)\exp(ik_z z)}{(k_z - \beta_{\text{spp}}) - i(\alpha_l + \alpha_{\text{spp}})}\mathrm{d}k_z, \tag{2a}$$

$$R \equiv \frac{s_{\text{out}}}{s_{\text{in}}} = e^{i\phi}\frac{(k_z - \beta_{\text{spp}}) + i\alpha_l - i\alpha_{\text{spp}}}{(k_z - \beta_{\text{spp}}) - i\alpha_l - i\alpha_{\text{spp}}}. \tag{2b}$$

Equation (2a) indicates that the amplitude of the excited SPP is sensitive to the phase of different incident wave-vector components $s_{\text{in}}(k_z)$. Particularly, the denominator of the integrand's denominator changes sign in its real part about β_{spp}. When the incident light is a conventional light beam such as a Gaussian beam, where $s_{\text{in}}(k_z)$ has linear phase variation about β_{spp}, the components with $k_z < \beta_{\text{spp}}$ and $k_z > \beta_{\text{spp}}$ have opposite contributions to the SPP excitation. As a result, a destructive interference arises, which strongly limits the peak intensity of the excited field. The analogous destructive interference also occurs in the time domain, where an excited state is subject to a conventional unchirped pulse in the applications of optically induced resonant transitions [7] and all-optical bistable switching [12]. Thus, in order to cancel out such destructive interference, a wave-vector-dependent phase modulation on s_{in} is required to balance the phase change around the SPP resonance:

$$\tilde{s}_{\text{in}} = s_{\text{in}}(k_z)\exp(i\ \arg[(k_z - \beta_{\text{spp}}) - i(\alpha_l + \alpha_{\text{spp}})]). \tag{3}$$

This phase modulation can be achieved experimentally through a $4f$ Fourier transformation system, where a transmissive spatial light modulator is positioned at the Fourier plane and modulates the phase for the different wave-vector components.

We numerically demonstrate this idea of enhancing the SPP excitation by a spatially modulated beam in a Kretschmann configuration [Fig. 1(a)], where the thickness of the silver layer is 58.3 nm, and the dielectric constant of the quartz prism is $\varepsilon_d = 2.25$. For silver, we assume a Drude permittivity dispersion $\varepsilon_m = \varepsilon_\infty - \omega_p^2/(\omega^2 + i\gamma_d\omega)$, $\varepsilon_\infty = 4.039$, $\omega_p = 1.391 \times 10^{16}$ rad · Hz, $\gamma_d = 3.139 \times 10^{13}$ rad · Hz, based on experimentally retrieved silver dispersion at the room temperature [23].

To determine the parameters of the spatial CMT theory, we fit Eq. (2b) to the amplitude and phase spectra of the reflection coefficients obtained from numerical simulation. Assuming that the wavelength of the incident light in free-space is $\lambda_0 = 632$ nm, the solid lines in Fig. 2 correspond to the amplitude and phase spectra of R, which are calculated by the transfer matrix method [24]. From Eq. (2b) we see that the phase of R should have a 2π shift as k_z changes from $k_z \ll \beta_{\text{spp}}$ to $k_z \gg \beta_{\text{spp}}$ when $\alpha_l > \alpha_{\text{spp}}$. In the range of $k_z = 1$–$1.06k_0$ ($k_0 = 2\pi/\lambda_0$),

the numerical simulation indicates that the phase of R indeed exhibits such a 2π shift. The theoretical results from Eq. (2), using the fitting parameters of $\phi = 0.97009$, $\beta_{\text{spp}} = 1.0301k_0$, $\alpha_{\text{spp}} = 4.5062 \times 10^{-4}k_0$, and $\alpha_l = 6.6990 \times 10^{-4}k_0$, are plotted as the dotted line in Fig. 2, which agree well with the numerical calculation. Also, β_{spp} as determined from the fit to the numerical simulation coincides with the wave vector of nonleaky SPP at the metal-air interface, i.e., $k_0\sqrt{\varepsilon_m/(1+\varepsilon_m)}$, and the very small deviation is due to the leakage of the SPP field.

The enhancement of SPP excitation is illustrated by a comparison between a conventional Gaussian illumination and the shaped beam after the phase modulation. We consider that the incident Gaussian beam has the magnetic field $H_y = H_0 \int s_{\text{in}}(k_z)\exp(ik_z z + ik_x x)\mathrm{d}k_z$, where H_0 is a normalization constant, $s_{\text{in}}(k_z) = \exp[-(k_z - \beta_{\text{spp}})^2/k_w^2]$, and $k_w = 0.0758k_0$. Such a Gaussian beam has a 2.652 μm radius waist and focuses at the quartz-metal surface, and the incident angle is 43.4°. Figures 3(a) and 3(b) are the amplitude and phase spectra for the Gaussian beam and the phase-shaped beam with the phase modulation of [Eq. (3)]. Figure 3(c) shows the incident magnetic field amplitude at the quartz-metal surface. Distinct from the Gaussian beam having a peak at the center, the magnetic field of the phase-shaped beam is zero at the center. Also the phase-shaped beam is much wider than the Gaussian beam and does not exhibit a symmetry profile about the center.

Figures 1(b) and 1(c) show the electric field intensity under the Gaussian beam and the phase-shaped beam illuminations. The fields are computed by using the superposition of the different spatial components applying the transfer matrix method to each spatial component. In comparison with the Gaussian beam, and the phase-shaped beam illumination the incident light efficiently tunnels through the metal layer and excites a SPP spot with much stronger intensity than that of the Gaussian beam. The intensities of the excited SPP at the surface $x = -0.06$ μm are plotted as the blue and green solid lines in Fig. 3(d) for the Gaussian beam and the phase-shaped beam illuminations, respectively. To compare with our spatial CMT, the red and cyan dotted lines in Fig. 3(d)

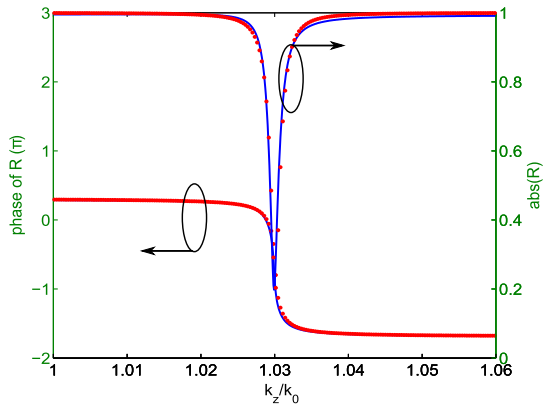

Fig. 2. Amplitude and phase spectra of the reflection coefficient in the Kretschmann configuration [Fig. 1(a)]. The solid line corresponds to the numerical calculation. The dotted line is the fitting result of the CMT Eq. (2b) with the parameters: $\phi = 0.97009$, $\beta_{\text{spp}} = 1.0301k_0$, $\alpha_{\text{spp}} = 4.5062 \times 10^{-4}k_0$, and $\alpha_l = 6.6990 \times 10^{-4}k_0$.

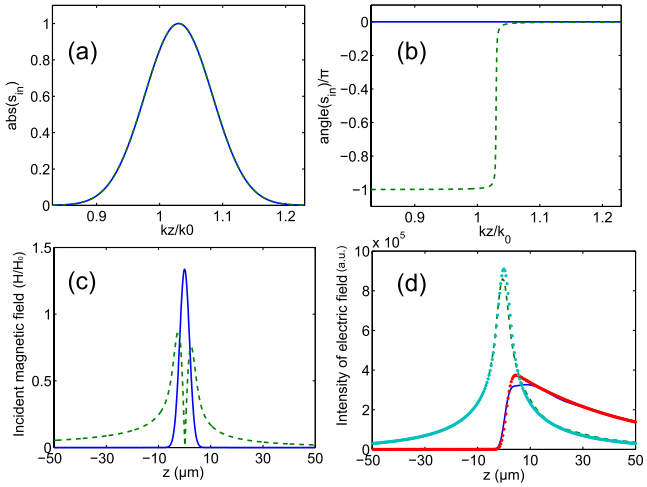

Fig. 3. (a),(b) Amplitude and phase spectra of the spatial components for the Gaussian beam (solid) and the phase-shaped beam Eq. (3) (dashed), respectively. (c) The magnetic field amplitude of the Gaussian beam (solid) and the phase-shaped beam (dashed) at the metal-quartz interface. (d) The electric intensity of the excitation SPP. The blue solid and green dashed lines correspond to Figs. 1(b) and 1(c) at $x = -0.06$ μm, respectively. The red and cyan dotted lines are computed by the CMT Eq. (2a) with the fitting parameters.

correspond to the intensity of excited SPP calculated by Eq. (2a) with the fitting parameters and the normalization process, which show good agreement between the CMT and the numerical simulation. As our theory predicts, the SPP field excited with the phase-shaped beam has a much higher peak intensity, and it is indeed more than 2.7-fold stronger than the conventional Gaussian illumination case. We note that the phase-shaped beam has the same incident power as the conventional Gaussian beam. More interestingly, the excited SPP field under the phase-shaped beam illumination is concentrated, and the hot energy spot has the full-width half-maximal about 10 μm and exhibits a symmetry profile about $z = 0$.

The proposed spatial control technology can be directly applied to three-dimensional (3D) beams which have a confined profile in the y direction. In these cases, Eq. (3) needs to take into account the wave-vector components in both the y and z directions. Figures 4(a) and 4(b) present the simulation results for the 3D p-polarized Gaussian beam and the phase-shaped beam through the modulation as Eq. (3), respectively. The excited SPP field by the phase-shaped beam still concentrates as a hot spot, and the peak intensity is 2.7 times the Gaussian beam illumination.

In summary, we propose that the SPP excitation on a metal surface can be strongly enhanced by the phase modulation on the incident illumination. We note that the field enhancement results from the constructive interference between different wave-vector components, while the launching efficiency and the propagation distance for the SPP mode of $k_z = \beta_{\text{spp}}$ are the same for both the conventional illumination and the phase-shaped beam. The proposed spatial control technique benefits the development of surface-enhanced applications. For example, in plasmon optical tweezers, a very high and

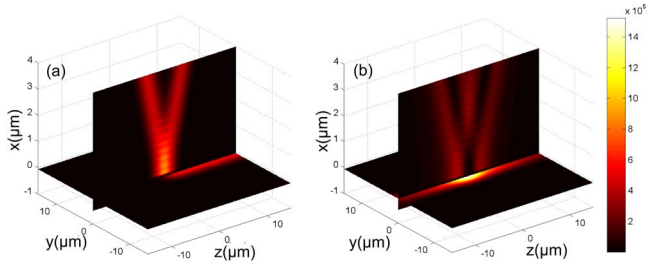

Fig. 4. Distribution of the electric field intensity $|\mathbf{E}|^2$ under the illumination of (a) the 3D p-polarization Gaussian beam and (b) the phase-shaped beam with the phase modulation of Eq. (3). The Gaussian beam has a 2.652 μm radius waist and focuses at the quartz-metal surface.

sharp field intensity of SPP excitation leads to strong optical gradient forces. Moreover, the phase shaping provides a new degree of freedom to fundamentally control the SPP excitation to move or sort micro-objects, and the spatial CMT is vital to design the phase modulation for a demanded intensity profile.

This work was financially supported by Fundamental Research Funds for the Central Universities (2014QNA3007). H. W. acknowledges the support from National Basic Research of China (grant 2013CB632702) and NSF of China (grant 51302141).

References

1. I. Vellekoop, A. Lagendijk, and A. Mosk, Nat. Photonics **4**, 320 (2010).
2. A. Derode, P. Roux, and M. Fink, Phys. Rev. Lett. **75**, 4206 (1995).
3. A. Sentenac and P. C. Chaumet, Phys. Rev. Lett. **101**, 013901 (2008).
4. B. Gjonaj, J. Aulbach, and P. M. Johnson, Nat. Photonics **5**, 360 (2011).
5. T. S. Kao, S. D. Jenkins, J. Ruostekoski, and N. I. Zheludev, Phys. Rev. Lett. **106**, 085501 (2011).
6. T. Weinacht, J. Ahn, and P. H. Bucksbaum, Nature **397**, 233 (1999).
7. N. Dudovich, D. Oron, and Y. Silberberg, Phys. Rev. Lett. **88**, 123004 (2002).
8. N. S. Ginsberg, S. R. Garner, and L. V. Hau, Nature **445**, 623 (2007).
9. M. I. Stockman, S. V. Faleev, and D. J. Bergman, Phys. Rev. Lett. **88**, 067402 (2002).
10. M. I. Stockman, D. J. Bergman, and T. Kobayashi, Phys. Rev. B **69**, 054202 (2004).
11. M. Aeschlimann, M. Bauer, D. Bayer, T. Brixner, F. J. G. de Abajo, W. Pfeiffer, M. Rohmer, C. Spindler, and F. Steeb, Nature **446**, 301 (2007).
12. S. Sandhu, M. L. Povinelli, and S. Fan, Appl. Phys. Lett. **96**, 231108 (2010).
13. S. A. Maier, *Plasmonics: Fundamentals and Applications* (Springer, 2007).
14. J. Homola, Chem. Rev. **108**, 462 (2008).
15. Y. Liu, S. Xu, X. Xuyang, B. Zhao, and W. Xu, J. Phys. Chem. Lett. **2**, 2218 (2011).
16. S. Palomba and L. Novotny, Phys. Rev. Lett. **101**, 056802 (2008).
17. J. Renger, R. Quidant, N. van Hulst, and L. Novotny, Phys. Rev. Lett. **104**, 046803 (2010).
18. N. B. Grosse, J. Heckmann, and U. Woggon, Phys. Rev. Lett. **108**, 136802 (2012).
19. G. Volpe, R. Quidant, G. Badenes, and D. Petrov, Phys. Rev. Lett. **96**, 238101 (2006).
20. M. Righini, A. S. Zelenina, C. Girard, and R. Quidant, Nat. Phys. **3**, 477 (2007).
21. M. L. Juan, M. Righini, and R. Quidant, Nat. Photonics **5**, 349 (2011).
22. H. Haus, *Waves and Fields in Optoelectronics* (Prentice-Hall, 1984).
23. P. B. Johnson and R. W. Christy, Phys. Rev. B **6**, 4370 (1972).
24. W. C. Chew, *Waves and Fields in Inhomogenous Media* (IEEE, 1995).